Chemical accelerator studies of reaction dynamics: $Ar^+ + CH_4 \rightarrow ArH^+ + CH_3$

J. R. Wyatt*, L. W. Strattan†, S. C. Snyder‡, and P. M. Hierl

Department of Chemistry, University of Kansas, Lawrence, Kansas 66045
(Received 4 May 1973)

Chemical accelerator studies on isotopic variants of the reaction $Ar^+ + CH_4 \rightarrow ArH^+ + CH_3$ are reported. Velocity and angular distributions of the ionic product as a function of initial translational energy have been measured over the energy range 0.39–25 eV center-of-mass (c.m.). The asymmetry of the product distribution with respect to the center of mass indicates that the reaction is predominantly direct over the energy range studied. The dynamics of the reaction are approximated by the spectator stripping model: The reaction exothermicity appears as product internal energy and product excitation increases with collision energy at the rate predicted by this model. The internal degrees of freedom of the neutral product have little effect on reaction dynamics, and product excitation appears to reside principally in the ionic product. Deviations from the spectator stripping model suggest the existence of a basin in the potential energy hypersurface for this reaction; the $ArCH_4^+$ complex which may be formed at low collision energies, however, preferentially decomposes via reaction channels other than that resulting in ArH^+ formation.

I. INTRODUCTION

In recent years beam techniques have been used to study the dynamics of ion–molecule reactions. Considerable attention has been given to intrinsically simple transfer reactions of the general type

$$X^+ + YZ \rightarrow XY^+ + Z \ , \tag{1}$$

where X is Ar, N_2, or CO, and YZ represents H_2, D_2, or HD.[1–9] These reactions have been found to proceed by a direct mechanism over the entire energy range studied (approximately 0.05–20 eV c.m.). At intermediate energies the simplest model of direct reaction, the spectator stripping model,[1,10] appears to provide a satisfactory description of the reaction mechanism, although deviations due to momentum and energy conservation have been found at higher energies ($\gtrsim 5$ eV).[2,3,5,6,11]

Deviations from spectator stripping also became significant at relative collision energies less than 2 eV.[3,4,7] The finding that the reaction products possess greater translational energy than expected on the basis of spectator stripping has been interpreted in terms of a simple model variously called "modified stripping,"[7] "polarization reflection,"[8] or "impulsive reaction."[12] This model, based on assumed long-range, intermolecular forces, has been used to account for product velocities,[7,8,13] energy partition,[7,8,13] angular distributions,[8,12] and isotope effects[7,14] in several simple hydrogen transfer reactions. A characteristic feature of this stripping-like model is the assumption that the dynamics of the reaction depend only upon the mass of spectator Z but not upon its internal structure, if any. However, this model has been compared with experimental results only for reactions in which an ion abstracts a hydrogen atom from molecular hydrogen.

Investigations at this laboratory have been designed to determine the extent to which the identity and nature of the spectator group affect the reaction dynamics. In particular, the reactions

$$Ar^+ + GH_4 \rightarrow ArH^+ + CH_3 \tag{2a}$$

$$Ar^+ + CD_4 \rightarrow ArD^+ + CD_3 \tag{2b}$$

were studied over the energy range 0.4–25 eV c.m. Velocity and angular distributions of the ionic products have been measured by chemical accelerator techniques. In addition, excitation function (reaction cross sections as a function of energy) have been measured and will be reported in detail in a future article. Preliminary results of Reaction (2a) have been published.[15]

Reaction (2) has previously been studied by high-pressure mass spectrometry[16] and by beam techniques.[17] In the latter study, Heglein and co-workers found that the reaction dynamics could be described by the spectator stripping model over a wide range of energy, although strongly unsymmetric broadening of the product ion velocity distribution together with a small shift in the center of gravity of the distribution to lower velocities occurred at collision energies less than 2 eV. This indication of a strong interaction between the incident ion and the CD_3 spectator group led Henglein to postulate a transition from the stripping mechanism at intermediate energies to the formation of a long-lived complex $ArCD_4^+$ at energies of a few tenths of 1 eV.[17] The present study confirms this low energy behavior of the product ion velocity distribution. It is shown, however, that this observation is consistent with a model for direct reactions.

The cross sections for Reactions (2) are about 100 times smaller than those for the corresponding reactions with H_2 and D_2.[15–17] The dominant reactions occurring in Ar^+–CH_4 mixtures are the asymmetric charge exchange reactions:

$$Ar^+ + CH_4 \rightarrow Ar + CH_4^+ \tag{3}$$

$$\rightarrow Ar + CH_3^+ + H \tag{4}$$

$$\rightarrow Ar + CH_2^+ + H_2 \ . \tag{5}$$

A rate constant $k_4 \sim 10^{-9}$ cc/mol · sec has been measured for Reaction (4), while k_5 and k_3 are about $\frac{1}{3}$ and $\frac{1}{9}$ of that value, respectively. No major changes in the relative yields have been found over a very wide range of collision energies.[18]

In a beam experiment in which the charge exchange products of Reactions (4) and (5) were energy analyzed,

 Copyright © 1975 American Institute of Physics

This article is copyrighted as indicated in the article. Reuse of AIP content is subject to the terms at: http://scitation.aip.org/termsconditions. Downloaded to IP: 129.237.46.100 On: Thu, 11 Sep 2014 20:24:30

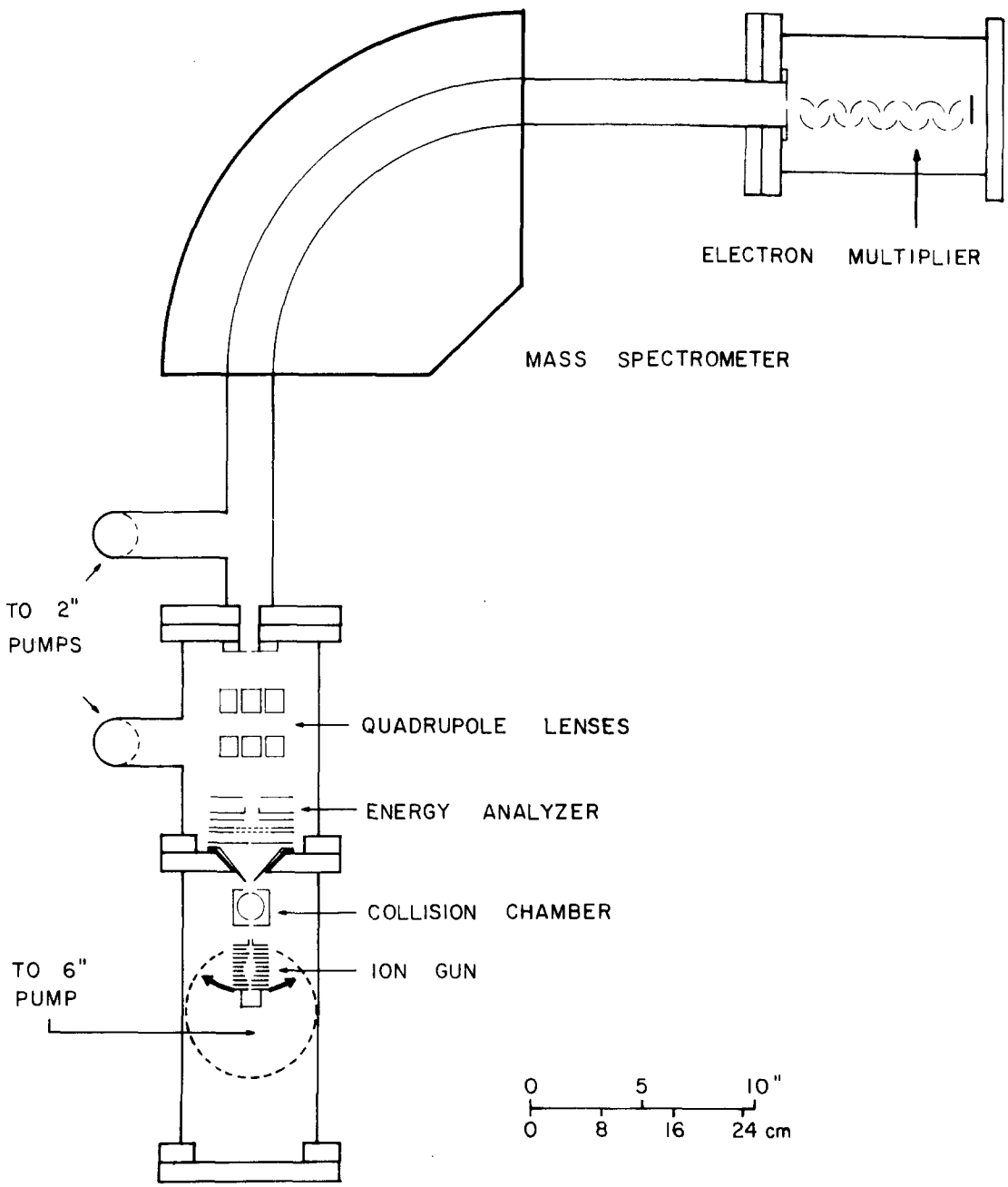

FIG. 1. Schematic representation of the instrument.

Henchman *et al.*[19] found that the reaction proceeds by two mechanisms, with and without momentum transfer. They suggest that the former involves the formation of a long-lived complex, while the latter proceeds directly via electron transfer at large inpact parameter.

The reactions

$$Ar^+ + CH_4 \rightarrow ArCH_2^+ + H_2 \quad (6)$$

$$\rightarrow ArCH_3^+ + H \quad (7)$$

are approximately 100 times slower[16] than Reaction (2) and were not observed in the present study.

II. EXPERIMENTAL

A. Apparatus

Figure 1 presents a schematic diagram of the chemical accelerator. Ions, formed by electron impact, are extracted, accelerated, and collimated by a system of electrostatic lenses.[20] The nearly monoenergetic ion beam of variable energy (0.50–100 eV LAB) passes through the collision chamber containing the neutral target gas, whose pressure ($\sim 10^{-3}$ Torr) is measured by a capacitance manometer and whose temperature (~85 °C) is measured by a thermocouple. The ion gun can be rotated about the center of the collision chamber, permitting the fixed detector to measure scattered products at various angles. Those ions leaving the collision cham-

This article is copyrighted as indicated in the article. Reuse of AIP content is subject to the terms at: http://scitation.aip.org/termsconditions. Downloaded to IP: 129.237.46.100 On: Thu, 11 Sep 2014 20:24:30

ber at the selected angle pass through a detection slit (typical resolution is 1° in the horizontal plane and 4° in the vertical), a stopping-potential energy analyzer, and a set of strong focusing quadrupole lenses.[21] Mass analysis of the ions is performed with a 30 cm, 90 degree deflection magnetic sector analyzer of a Nuclide mass spectrometer from which the conventional ion source and accelerating electrodes have been removed.

Energy analysis is accomplished by applying a modulated dc retarding potential to a retarding grid. This potential, in the form of a sawtooth wave (11 Hz), generates a complete energy spectrum every 0.09 sec, thus permitting continuous display of the entire energy spectrum on an oscilliscope as well as providing a repetitive signal for signal averaging with a Varian C-1024 signal averaging computer.

The individual components of this instrument are described in detail elsewhere.[22]

B. Internal states of the reactants

The Ar^+ is produced by impact of 40 eV electrons, so that the primary ion beam contains no doubly charged ions[23] and less than 1% high energy metastable ions.[24] The remaining 99% are in the ^2P state and should be distributed statistically in a 2:1 ratio between the $J=\frac{3}{2}$ and the $J=\frac{1}{2}$ levels, which differ in energy by 0.18 eV.

The neutral target gas is assumed to be in thermal equilibrium, so that the internal energy of the molecular reactant is determined by the temperature of the gas. Since the temperature is 85 °C under the conditions of the experiment, nearly all of the CH_4 and CD_4 molecules are in their ground vibrational state. The most probable rotational states are $J=6$ for CD_4 and $J=9$ for CH_4, which correspond to an energy of about 0.015 eV for either molecule. Consequently, most of the energy possessed by the products must come from the heat of reaction.

Intermolecular potentials for ArH^+, derived from the inversion of elastic scattering data, indicate that the well depth D_e is 4.10 ± 0.10 eV (with respect to dissociation into Ar and H^+) and that the equilibrium internuclear distance r_e is 1.33 ± 0.05 Å.[25] Similar results have been obtained from *ab initio* calculations.[26] The zero point vibrational energy of ArH^+ inferred from the form of the ArH^+ potential energy curve[25b] is approximately 0.20 eV. (This compares with 0.18 eV for the isoelectronic molecule HCl.) Consequently, the dissociation energy $D_0(Ar-H^+) \cong 3.90$ eV, resulting in energies of 6.06 and 6.24 eV for dissociation of ArH^+ into $Ar^+(^2P_{3/2}) + H$ and $Ar^+(^2P_{1/2}) + H$, respectively. With a value of $D(H-CH_3) = 4.406$ eV,[27] the following reaction enthalpies are obtained:

$$Ar^+(^2P_{3/2}) + CH_4(^1A_1) \rightarrow ArH^+(X^1\Sigma^+) + CH_3(^2A_2'')$$
$$\Delta H = -1.65 \text{ eV} \quad (8a)$$

$$Ar^+(^2P_{1/2}) + CH_4(^1A_1) \rightarrow ArH^+(X^1\Sigma^+) + CH_3(^2A_2'')$$
$$\Delta H = -1.83 \text{ eV} . \quad (8b)$$

Since, in the present experiment, the reactant Ar^+ ions are distributed between the $^2P_{3/2}$ and $^2P_{1/2}$ states, we have used the statistical weighting factor of 2:1 to arrive at a weighted average for the heat of reaction, $\Delta H = 1.71$ eV.[28]

III. RESULTS

Angular (Θ) distributions in the laboratory (LAB) system are obtained by recording the ion signal while rotating the ion gun about the center of the collision chamber. Because the detector views a decreasing fraction of the collision path length with increasing angle, the observed ion signal at each laboratory angle is divided by the path length subtended by the detector at that angle. The reported angular distributions, $I_L(\Theta, \Phi = 0)$, which are normalized to unity at the angular maximum, therefore represent the relative ion intensity scattered through a laboratory angle Θ in the plane $\Phi = 0$ from a reaction path of unit length. Typical results are shown in Fig. 2(a).

The stopping potential curves obtained at various angles are first scaled to reflect the total relative intensity at that angle and are then differentiated to yield the energy distribution at that angle, $I_L(E, \Theta, \Phi = 0)$. These energy distributions are transformed to velocity distributions by multiplying each point by the corresponding laboratory velocity v in accord with the transformation

$$I_L(E, \Theta, \Phi)\, dE\, d\Omega = I_L(v, \Theta, \Phi)\, dv\, d\Omega . \quad (9)$$

This yields the relative differential cross section for scattering into the solid angle $d\Omega$, located at angles Θ and Φ, with velocity between v and $v + dv$. Typical results are shown in Fig. 2(b).

The laboratory cross sections, $I_L(v, \Theta, \Phi)$, are converted to probabilities in Cartesian velocity space according to the transformation

$$P_C(v_x, v_y, v_z) = v^{-2} I_L(v, \Theta, \Phi) , \quad (10)$$

where P_C represents the probability of finding product in a given volume of velocity space.[8,29] These probabilities are then scaled, with the highest intensity arbitrarily set equal to 100. A plot of the appropriate contours on a velocity vector diagram produces a map of relative intensities as seen by a detector sensitive to particles in an element $dv_x dv_y dv_z$ of velocity space.

From data such as that shown in Fig. 2, velocity vector diagrams have been constructed to present Cartesian probabilities of ArH^+ (shown in Figs. 3–6) and ArD^+ (not shown) formed in Reaction (2) at several energies of the Ar^+ beam.

Since, for the purpose of this investigation, the position of the maximum of the product ion intensity was of interest, another technique was employed as an alternative to the construction of the complete velocity vector diagram. The product ion angular distribution was scanned to determine the angle of maximum intensity, and the energy distribution was then measured at the angle of maximum product ion intensity. This energy spectrum was converted to the corresponding Cartesian spectrum by multiplying the intensity at each point by the overall Jacobian factor of $1/v$. The results are contained in Table I, which lists the laboratory energy of the Ar^+ and the laboratory energy of the product ion cor-

This article is copyrighted as indicated in the article. Reuse of AIP content is subject to the terms at: http://scitation.aip.org/termsconditions. Downloaded to IP: 129.237.46.100 On: Thu, 11 Sep 2014 20:24:30

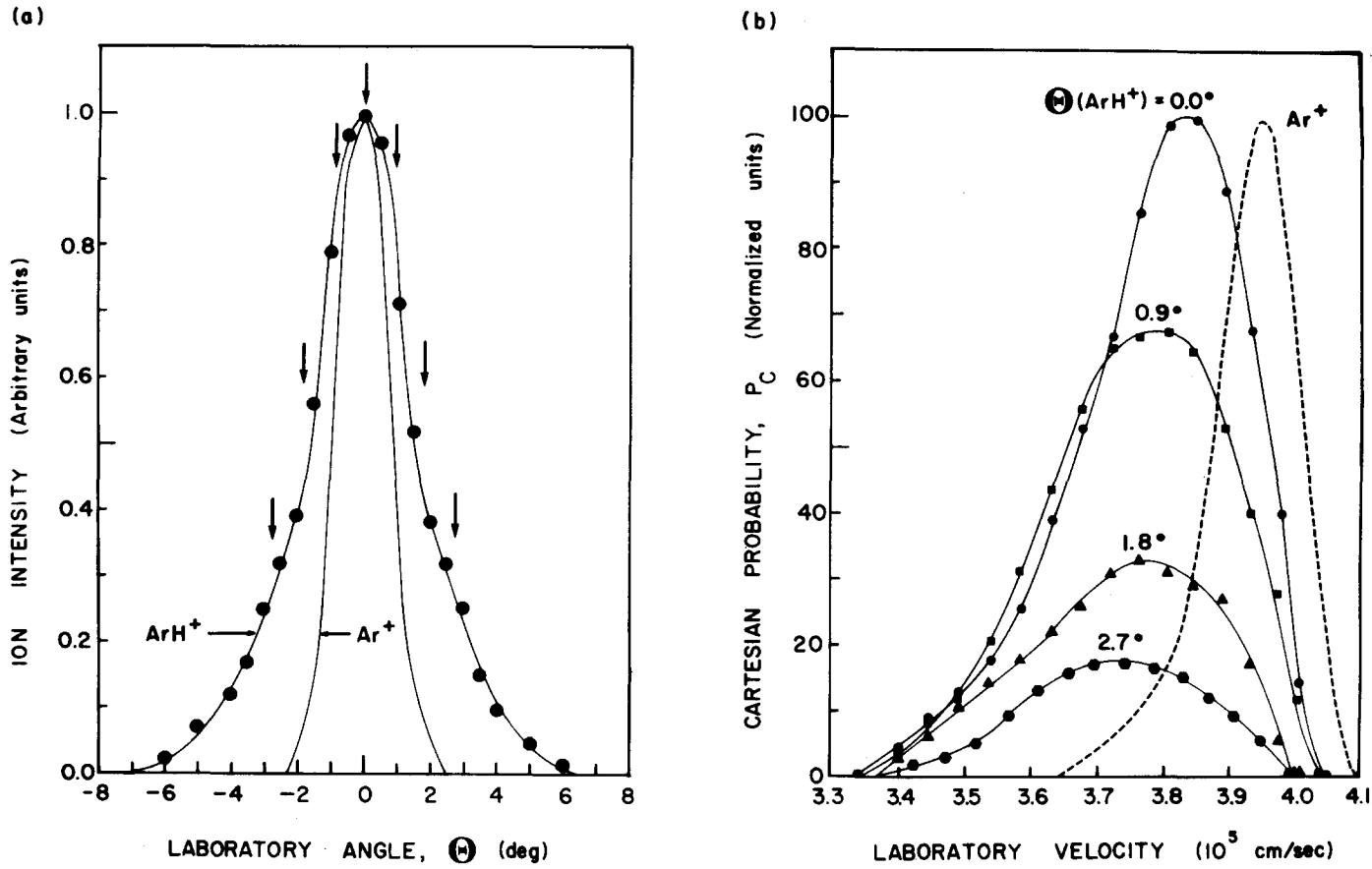

FIG. 2. Data on $Ar^+ + CH_4 \rightarrow ArH^+ + CH_3$ at laboratory energy $E(Ar^+) = 3.22$ eV. (a) Angular distributions are normalized to unity for both reactant and product ions. Representative data (closed circles) are shown for the product distribution, which was corrected for angular dependence of reaction path subtended by detector. Arrows indicate angles at which product energy distributions were measured. (b) Velocity spectra for reactant ion at $\Theta = 0°$ (dashed line) and for product ion at indicated laboratory angles. Areas under each curve correspond to total relative intensity at the given angle. For the sake of clarity, velocity spectra for product ion at negative angles have been omitted from Fig. 2(b).

responding to the peak in its Cartesian velocity spectrum. The translational exoergicity and the ratio of the center of mass velocity of the ionic product to the center of mass velocity of the Ar^+, u^*_{ArH}/u^*_{Ar}, are presented in Table I, and are plotted vs the center of mass collision energy in Figs. 7 and 8, respectively.

IV. DISCUSSION

A. Direct mechanism vs long-lived intermediate

If the reaction proceeded by the formation on an intermediate that persisted for at least several rotational periods (only about 10^{-13} sec at these energies), the product distribution would necessarily be symmetric with respect to a plane passing through the center of mass and perpendicular to the relative velocity vector.[30] Product velocity vector distributions for Reaction (2a) at four different collision energies are shown in Figs. 3–6. (Because no product intensity was observed behind the center of mass, this region of velocity space has been omitted from the figures.) The observed asymmetry about $\pm 90°$ in the c.m. system is a clear indication that, even at the lowest energy measured (0.92 eV c.m.), the contribution of any long-lived intermediate is small, and that the reaction is dominated by a direct mechanism (i.e., an impulsive type of interaction occurring on a time scale comparable to one rotational period).

While the product distribution clearly remains forward peaked as the collision energy is decreased, there is increased broadening of the distribution and the formation

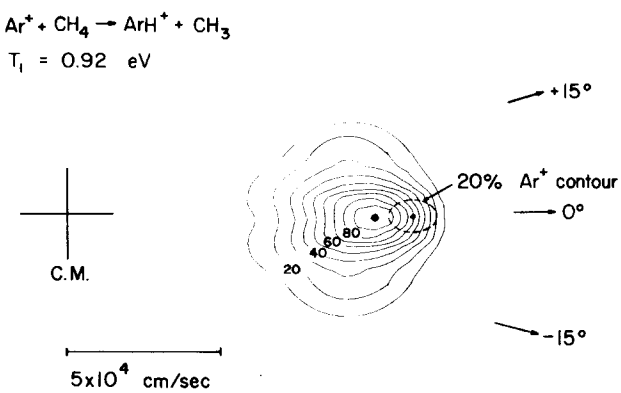

FIG. 3. Product probability distribution for Reaction (2a) at the collision energy $T_1 = 0.92$ eV (c.m.). The product ion intensities, normalized to 100 at the position of maximum intensity, are shown relative to the Cartesian system P_C. Arrows represent scattering angle with respect to the center of mass (marked C.M.). The dashed oval represents the 20% contour line for the reactant Ar^+.

This article is copyrighted as indicated in the article. Reuse of AIP content is subject to the terms at: http://scitation.aip.org/termsconditions. Downloaded to IP: 129.237.46.100 On: Thu, 11 Sep 2014 20:24:30

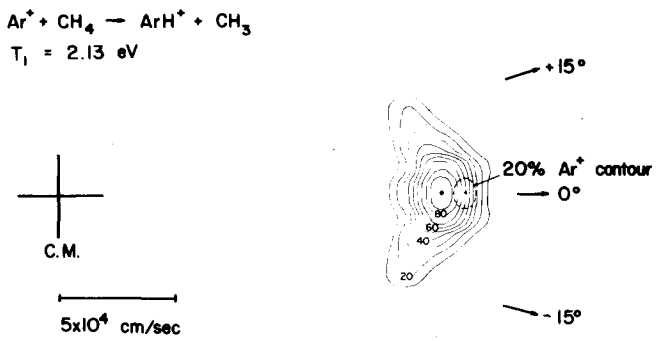

FIG. 4. Product probability distribution for Reaction (2a) at the collision energy $T_1 = 2.13$ eV (c. m.).

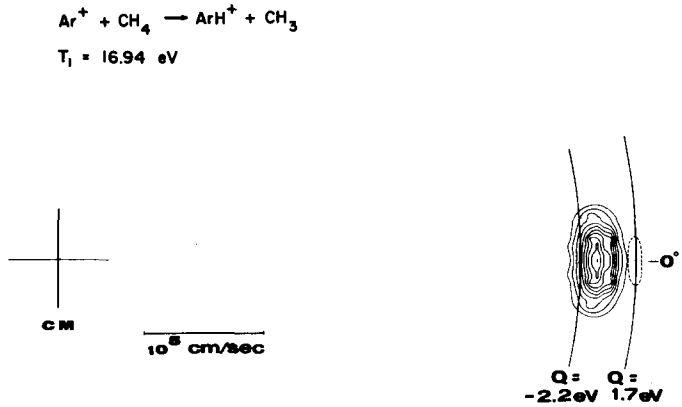

FIG. 6. Product probability distribution for Reaction (2a) at the collision energy $T_1 = 16.94$ eV (c. m.). The contour lines, unlabelled for the sake of clarity, have the same significance as in the preceding figures.

of a low-velocity tail extending toward the center of mass (see Fig. 3). Similar observations were reported by Henglein,[17] who interpreted this phenomenon as indicating an increasing degree of interaction between the incident ion and the CH_3 group at the lower collision energies. Extrapolating this behavior to even lower energies, Henglein suggested this tailing indicated a transition from a direct mechanism at higher energies to a long-lived complex mechanism at lower energies. If, however, ArH^+ production involved the formation of a complex that rotated at least once before decomposing, the ArH^+ distribution would show a back-scattered peak resulting from those complexes which lived $n+\frac{1}{2}$ rotational periods, where n is an integer. Such behavior has been reported for the reaction of $C_2H_4^+$ with C_2H_4.[31] For this reaction at energies ≥ 8 eV c. m., the $C_3H_5^+$ product is forward peaked. At intermediate energies (~4 eV c. m.) a second peak in the product distribution occurs as far behind the center of mass as the principal peak is forward. As the collision energy is further decreased, the two peaks become more nearly equal in magnitude, until at collision energies ~1.4 eV the product distribution is symmetrically distributed about the c. m. The present results show no such back-scattered peak and hence provide no evidence whatsoever for the production of ArH^+ via the formation of a persistent intermediate complex (defined as an entity in which all atoms are bound at reasonably normal bond distances for at least one rotational period).

The observed low-energy tailing presumably arises from two effects. First, the energy spread of the primary ion beam and the Maxwellian distribution of velocities for the target molecules give rise to a distribution of centroids rather than a single, unique center of mass. This effect will be most noticeable at low collision energies, where the thermal motion of the target molecules contributes significantly to the relative velocity.

Secondly, the strong intermolecular forces between an ion and a polarizable molecule cannot be neglected when the collision energy is comparable to or less than the

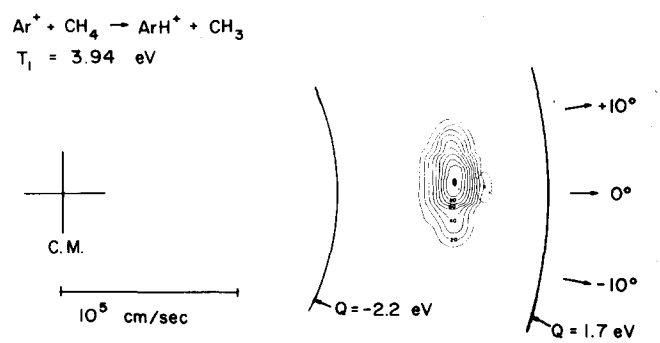

FIG. 5. Product probability distribution for Reaction (2a) at the collision energy $T_1 = 3.94$ eV (c. m.). The arcs marked $Q = 1.7$ eV and -2.2 eV represent the c. m. velocities of ArH^+ that correspond to zero and to maximum internal excitation of ArH^+. See Eq. (14) and the subsequent portion of the text for more information concerning these values.

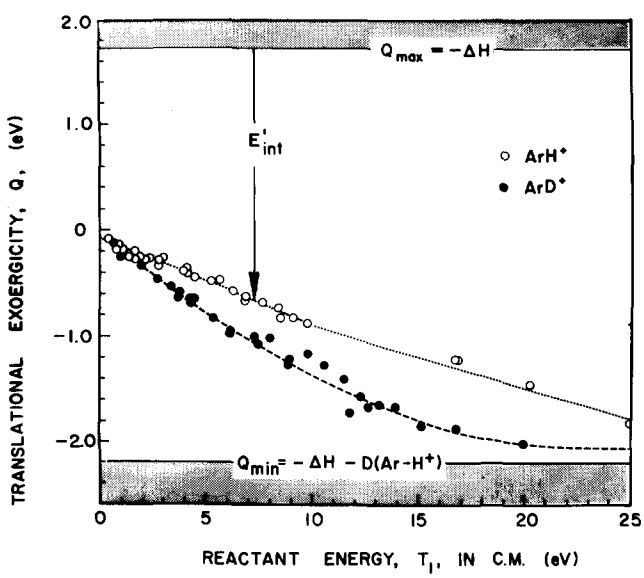

FIG. 7. Translational exoergicity Q vs initial relative energy T_1 for reactions of Ar^+ with CH_4 (○) and with CD_4 (●) over the energy range 0–25 eV c. m. (Many low energy points are omitted for the sake of clarity. They are included in Fig. 10). Lines drawn through data points represent best fit to experimental results. Upper limit Q_{max} is determined by energy released in reaction, $-\Delta H \cong 1.7$ eV. Lower limit Q_{min} is determined by the dissociation energy of ArH^+ and the assumption that all of the product internal excitation resides in the ionic product.

This article is copyrighted as indicated in the article. Reuse of AIP content is subject to the terms at: http://scitation.aip.org/termsconditions. Downloaded to IP: 129.237.46.100 On: Thu, 11 Sep 2014 20:24:30

TABLE I. Data for reactions of the type $X^+ + YZ \rightarrow XY^+ + Z$.

Most probable lab energy of X^+ (eV)	Most probable lab energy of XY^+ (eV)	Collision energy, T_1 (eV)	Translational exoergicity, Q (eV)	Velocity ratio, u_{XY^+}/u_{X^+}
A. $Ar^+ + CH_4 \rightarrow ArH^+ + CH_3$				
1.380	1.321	0.394	−0.087	0.852
1.410	1.321	0.403	−0.087	0.846
1.739	1.648	0.497	−0.089	0.867
1.966	1.896	0.562	−0.070	0.895
2.770	2.578	0.791	−0.187	0.836
3.217	3.077	0.919	−0.139	0.881
3.717	3.563	1.062	−0.153	0.884
3.799	3.573	1.085	−0.223	0.853
4.757	4.502	1.359	−0.252	0.863
5.522	5.275	1.578	−0.257	0.883
5.869	5.671	1.677	−0.198	0.899
6.759	6.507	1.931	−0.251	0.892
6.923	6.652	1.978	−0.270	0.889
7.514	7.252	2.147	−0.262	0.897
8.090	7.860	2.311	−0.230	0.908
9.635	9.309	2.753	−0.326	0.898
9.950	9.664	2.843	−0.286	0.907
10.45	10.20	2.987	−0.250	0.916
13.81	13.41	3.944	−0.391	0.908
14.38	13.98	4.109	−0.400	0.909
14.59	14.23	4.170	−0.365	0.914
15.80	15.37	4.513	−0.426	0.910
18.48	18.00	5.279	−0.475	0.912
19.53	19.08	5.580	−0.457	0.917
21.45	20.86	6.130	−0.591	0.909
24.13	23.45	6.895	−0.679	0.908
24.16	23.56	6.904	−0.608	0.913
26.82	26.14	7.664	−0.684	0.913
29.40	28.67	8.399	−0.725	0.914
29.74	28.85	8.500	−0.816	0.909
32.03	31.21	9.152	−0.820	0.912
34.34	33.46	9.810	−0.873	0.913
59.29	58.09	16.94	−1.20	0.921
59.33	58.12	16.95	−1.21	0.921
70.38	68.98	20.11	−1.43	0.921
89.99	88.17	25.71	−1.81	0.922
B. $Ar^+ + CD_4 \rightarrow ArD^+ + CD_3$				
1.973	1.898	0.658	−0.076	0.871
1.977	1.872	0.659	−0.105	0.849
2.893	2.651	0.964	−0.240	0.803
3.663	3.413	1.021	−0.250	0.826
3.806	3.563	1.269	−0.242	0.833
3.846	3.625	1.282	−0.221	0.843
6.037	5.732	2.012	−0.304	0.853
8.309	7.830	2.770	−0.479	0.842
10.30	9.797	3.434	−0.506	0.855
11.05	10.39	3.682	−0.654	0.840
11.38	10.81	3.793	−0.563	0.855
12.70	12.04	4.234	−0.658	0.851
12.83	12.14	4.276	−0.684	0.849
13.72	13.08	4.574	−0.645	0.860
16.23	15.41	5.409	−0.814	0.854
16.33	15.50	5.444	−0.832	0.852
18.51	17.53	6.169	−0.974	0.850
18.67	17.64	6.224	−0.908	0.856
19.51	18.59	6.503	−0.915	0.858
21.76	20.76	7.252	−1.000	0.859
22.66	21.57	7.553	−1.086	0.857
24.17	23.14	8.049	−1.010	0.866
26.46	25.19	8.819	−1.270	0.857
26.82	25.60	8.940	−1.222	0.860
29.22	28.08	9.740	−1.137	0.870
31.98	30.71	10.66	−1.264	0.869
34.51	33.11	11.50	−1.402	0.868
34.96	33.27	11.65	−1.734	0.856
37.02	35.45	12.34	−1.572	0.865
38.06	36.37	12.69	−1.697	0.885
39.36	37.71	13.12	−1.643	0.866
41.89	40.256	13.96	−1.627	0.869
45.32	43.48	15.11	−1.832	0.868
50.51	48.67	16.84	−1.840	0.874
60.70	58.68	20.23	−2.009	0.879
C. $Ar^+ + CH_2D_2 \rightarrow ArH^+ + CHD_2$				
3.579	3.395	1.111	−0.182	0.878
13.00	12.60	4.035	−0.400	0.911
24.18	23.54	7.505	−0.645	0.912
D. $Ar^+ + CH_2D_2 \rightarrow ArD^+ + CH_2D$				
3.579	3.358	1.111	−0.220	0.824
13.00	12.35	4.035	−0.653	0.843
24.18	23.02	7.505	−1.163	0.846

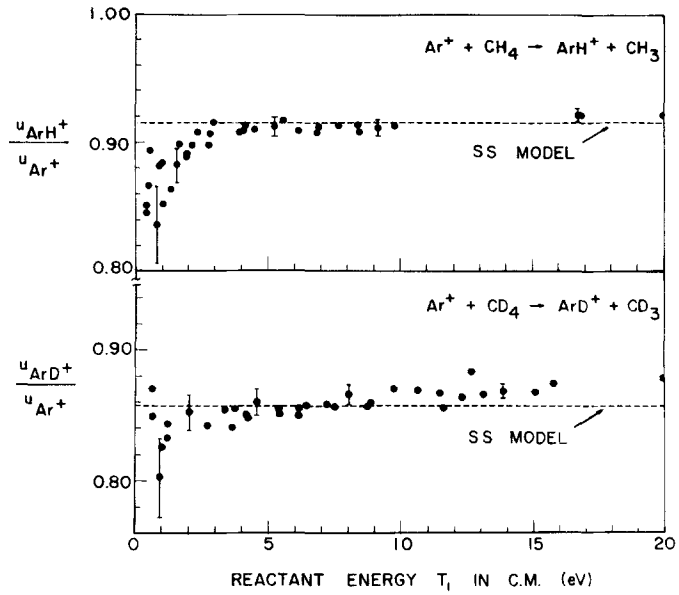

FIG. 8. Ratio of the center of mass velocity of the ionic product to the center of mass velocity of the Ar^+ reactant, u_{ArH}/u_{Ar^+}, vs initial relative energy T_1 for reaction of Ar^+ with (a) CH_4 and with (b) CD_4. The product ion velocities are determined from the position of maximum probability in Cartesian system P_C. Dashed line represents velocity ratio predicted by spectator stripping (SS) model, Eq. (16).

ion-induced dipole potential (i.e., several tenths of an eV). Because of this attractive force, the reactants will follow curved trajectories rather than rectilinear ones. The products will be distributed forwards, sideways, or even backwards, depending upon the degree of curvature.[32] As a result, the product distributions may broaden or even display a degree of forward-backward symmetry, thus presenting the appearance of a long-lived intermediate although no such persistent complex is actually involved in the formation of the observed product.

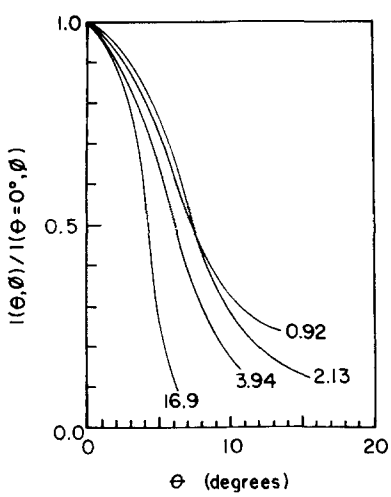

FIG. 9. The reduced differential cross sections $I(\theta, \phi)/(\theta = 0°, \phi)$ for formation of ArH^+ as a function of the center-of-mass scattering angle θ. The labels on the curves give the values of the c.m. collision energy in eV.

This article is copyrighted as indicated in the article. Reuse of AIP content is subject to the terms at: http://scitation.aip.org/termsconditions. Downloaded to IP: 129.237.46.100 On: Thu, 11 Sep 2014 20:24:30

Differential cross sections, $I(\theta, \phi)$, were calculated from the four velocity vector diagrams shown (Figs. 3–6) using the relation

$$I(\theta, \phi) = \int_0^\infty P_C(u, \theta, \phi) u^2 du \ , \tag{11}$$

where $P_C(u, \theta, \phi) = P_C(v_x, v_y, v_z)$, and where u, θ, and ϕ refer to the ArH^+ velocity and scattering angles in the center of mass coordinate system. The reduced differential cross sections, $I(\theta, \phi)/I(\theta = 0^0, \phi)$, are shown in Fig. 9. The angular distributions became narrower as the collision energy increased, suggesting the H-atom abstraction, at least at the higher energies employed in this study, occurs principally in grazing encounters resulting from moderately large impact parameter collisions. The broadening observed at the lower collision energies presumably reflects the increased curvature in the trajectories introduced by the intermolecular potentials, as discussed in the preceeding paragraph.

In this respect, it is interesting to note that trajectory studies[33] of the hot-atom reaction

$$T + CH_4 = TH + CH_3 \tag{12}$$

have indicated that this reaction is direct (i.e., the extension of the broken C–H bond is continuous during the reaction event, without back-tracking) and concerted (i.e., all three particles interact simultaneously, instead of sequentially in pairs).[34] Moreover, the product scattering distributions were found to be peaked sideways or slightly forward at low collision energies, more strongly forward peaked at higher energies, and to have a correlation between impact parameter and scattering angle.

B. Energy partitioning

The partitioning of reaction energy between internal and translational modes can be expressed in terms of the translational exoergicity Q, defined as the net difference between the final and initial kinetic energies,

$$Q = T_2 - T_1 \ . \tag{13}$$

Conservation of energy requires that the internal energy residing in the reaction products be given by

$$E'_{int} = E_{int} - Q - \Delta H \ . \tag{14}$$

For the reactions studied here, the internal energy of the reactants may be neglected, so that $E'_{int} \cong 1.71 - Q$ (eV). The greatest possible value of Q occurs when all available energy appears as product translation (i.e., when $E'_{int} = 0$): $Q_{max} = -\Delta H = 1.71$ eV. A pseudominimum value for Q can be assigned if one assumes all product excitation is contained in the ionic product. In this case, E'_{int} must be less than $D_0(Ar - H^+)$ for stable product formation. Thus, $Q_{min} = -D_0(Ar - H^+) - \Delta H = -2.19$ eV. Observation of ArH^+ at Q values more negative than Q_{min} requires that the CH_3 be internally excited.

Q values that correspond to the point of peak intensity in the Cartesian velocity spectra are listed in Table I and displayed vs collision energy T_1 in Fig. 7. From these data one can draw three conclusions concerning the "most probable" reaction mechanism.

(1) There is a net conversion of translational energy into internal energy (i.e., $Q < 0$) at all collision energies. Consequently, the entire heat of reaction appears as internal energy of the reaction products. This contrasts with the results obtained for reactions of Ar^+, N_2^+, and CO^+ with H_2 (or D_2), in which a small fraction of the reaction exothermicity is converted to translational energy at the lowest collision energies ($T_1 \lesssim 0.3$ eV).[35]

(2) As the collision energy T_1 increases, Q becomes more negative, indicating increased internal excitation of the products. Moreover, this conversion of translational energy to internal energy is more pronounced for reaction with CD_4 than for reaction with CH_4; that is, in reactions at the same energy in the center of mass system, the products of Reaction (2b) possess greater internal excitation than do the products of Reaction (2a). This behavior is also demonstrated by the reactions

$$Ar^+ + CH_2D_2 \rightarrow ArH^+ + CHD_2 \tag{15a}$$

$$\rightarrow ArD^+ + CH_2D \ . \tag{15b}$$

At a given collision energy, Q is more negative for ArD^+ than for ArH^+ (see Table I), indicating that the products of Reaction (15b) possess greater internal energy than do the products of Reaction (15a).

(3) Although the translational exoergicity Q decreases linearly with increasing reactant energy in the low and intermediate energy region, it becomes independent of T_1 at high energies. The limiting value of Q is about -2.0 eV, which corresponds to $E'_{int} \cong 3.7$ eV, a value close to the dissociation limit of ArH^+. This suggests that all of the internal excitation resides in the ionic product, so that the asymptotic approach to $Q \sim -2.0$ eV is caused by excitation of ArH^+ to its dissociation limit. This explanation has been proposed to account for similar behavior in several other ion–molecule reactions.[2,5,6,22,36,37] In these previously studied reactions the neutral product has always been monatomic and hence incapable of internal excitation (other than electronic). A polyatomic neutral product such as CH_3, on the other hand, has internal degrees of freedom which could possess a significant fraction of the available energy and thereby permit E'_{int} to be greater than the dissociation limit of the ionic product. The present results, however, strongly suggest that the "most probable" process does not involve the transfer of reaction energy of the internal degrees of freedom of the methyl fragment.

In this respect, it is interesting to compare the present results with those obtained for the abstractions of hydrogen from methane by halogen atoms. Although Cl is isoelectronic with Ar^+, the latter is considerably more electrophilic because of its far greater electron deficiency and might, therefore, be more comparable to F in terms of reactivity.[38] In chemical laser studies of the partitioning of reaction energy, Pimental and co-workers[41] found that $F-CH_4$ and $F-H_2$ systems gave remarkably similar vibrational energy distributions, with nearly all of the available energy appearing in the HF product. The CH_3 product, therefore, was formed in its ground state planar configuration. Lee *et al.*,[42] have

This article is copyrighted as indicated in the article. Reuse of AIP content is subject to the terms at: http://scitation.aip.org/termsconditions. Downloaded to IP: 129.237.46.100 On: Thu, 11 Sep 2014 20:24:30

found similar energy partitioning in molecular beam studies of the reaction $F + C_2D_4 \rightarrow DF + C_2D_3$.

It should be noted, however, that the contour map at $T_1 = 16.94$ (Fig. 6) shows some product intensity at Q values more negative than the pseudolimit of -2.2 eV. Similar behavior occurred in a contour map (not shown) for Reaction (2b) at a collision energy of 12.67 eV. Since product intensity can appear in this region of velocity space only if the neutral product contains some internal excitation, it is clear such excitation plays an important role in product stabilization, at least in the higher energy collisions. Significant internal excitation of CH_3 at high collision energies has been reported by Mahan and co-workers[43] for the reaction of N_2^+ with CH_4.

C. Spectator stripping mechanism

The spectator stripping (SS) mechanism, the simplest model for direct reactions, assumes that ion X^+ reacts impulsively with the transferred atom Y. The freed particle Z acts merely as a spectator to the reaction, proceeding after reaction with a velocity unchanged from that of the YZ reactant. The kinematics of the spectator stripping process lead to the prediction that the ratio of the c.m. velocity of the ionic product u_{XY}^+ to the c.m. velocity of the ionic reactant u_X^+ is

$$\left(\frac{u_{XY}^+}{u_X^+}\right)_{SS} = \frac{(X)(Z)}{(X+Y)(Z+Y)}, \tag{16}$$

where (i) represents the mass of particle i. Thus the velocity ratio should be a constant that depends only upon the masses of the particles. This ratio equals 0.915 for reaction of Ar^+ with CH_4 and 0.857 for reaction with CD_4.

Experimentally determined values for the velocity ratio are listed in Table I and are presented graphically in Fig. 8. The experimental values (determined from the peak in the Cartesian velocity spectra) agree reasonably well with the predictions of the SS model at the higher collision energies ($T_1 \gtrsim 2$–3 eV), but as the collision energy decreases the product ion appears at c.m. velocities progressively smaller then expected on the basis of the SS model. Similar results have been reported by Henglein and co-workers.[17] The direction of these low-energy deviations is exactly the opposite from the behavior observed for the reactions with hydrogen.[7] Consequently, Henglein has suggested that these deviations indicate a transition from a direct mechanism at high energies to a complex mechanism at low energies. However, it will be shown that the same mechanism proposed to explain the increases in the u_{XY}^+/u_X^+ ratio for hydrogen reactions can explain a decrease in this ratio for methane reactions.

D. Modified stripping

It has been suggested[7] that the failure of the SS model is due to the fact that it ignores all intermolecular forces (except, of course, to recognize that they cause the transfer process itself). Accordingly, this model has been modified by considering the effects of intermolecular potentials on the dynamics of direct reactions. This modified model states that the reactants experience a long-range attractive force which accelerates them towards each other so that at distance of closest approach their relative velocity is greater than it had been at infinite separation. It is assumed that transfer occurs in a direct manner at this distance of closest approach, with the products retaining some fraction f of the relative translational energy the reactants had immediately prior to transfer. The products then recede from each other, being decelerated (or accelerated) by the attractive (or repulsive) forces between them. These models predict that the translational exoergicity should vary with the collision energy according to the equation

$$Q = Q_0 + (f-1)T_1 . \tag{17}$$

This model, first proposed by Smith,[44] states that Q_0 (the translational exoergicity extrapolated to zero initial energy) is given by

$$Q_0 = fP + P' , \tag{18}$$

where P is the potential energy converted into translational energy as the reactants are brought from infinite separation to the distance at which transfer occurs, and P' is the potential energy released as kinetic energy as the products separate. Smith equated f with $\cos^2\beta$, where β is the angle between the skewed axes of the potential energy surface on which a sliding mass point represents the progress of the collision (this assumes specular reflection of the mass point). Bunker[45] subsequently obtained an expression for $\cos^2\beta$ in terms of the relative masses of the species involved and the angle of attack α, and showed that in the special case of collinear approach this factor reduced to the simple expression given by the spectator stripping model; that is,

$$\cos^2\beta = \frac{(X)(Z)}{(X+Y)(Z+Y)} \quad (\text{when } \alpha = \pi) . \tag{19}$$

In general, however, $\cos^2\beta$ varies between 0 and the value given by Eq. (19) as α varies between 0 and π. Consequently, potential energy P, released as the reactants approach, will appear, in large part, as vibrational energy of the newly formed XY bond; energy P', released as the products separate, will appear as product translation. This prediction has been confirmed in trajectory studies on assumed potential energy surfaces: attractive or "early downhill" surfaces ($P > P'$) resulted in high product vibration, while repulsive or "late downhill" surfaces ($P < P'$) resulted in product translation.[46]

Quantitative application of this model requires the evaluation of the potential energy terms P and P'. Because accurate potential energy surfaces are frequently not available, simplified expressions such as $P = -\alpha e^2/2r^4$ have been used[7,8] to describe the potential between an ion and a polarizable molecule. Such representations are of questionable accuracy and are not necessary for the purpose of this discussion.

Figure 10 shows the most probable value of the translational exoergicity plotted as a function of collision energy for Reactions (2a) and (2b) over the low and intermediate energy region, where this model may be ex-

This article is copyrighted as indicated in the article. Reuse of AIP content is subject to the terms at: http://scitation.aip.org/termsconditions. Downloaded to IP: 129.237.46.100 On: Thu, 11 Sep 2014 20:24:30

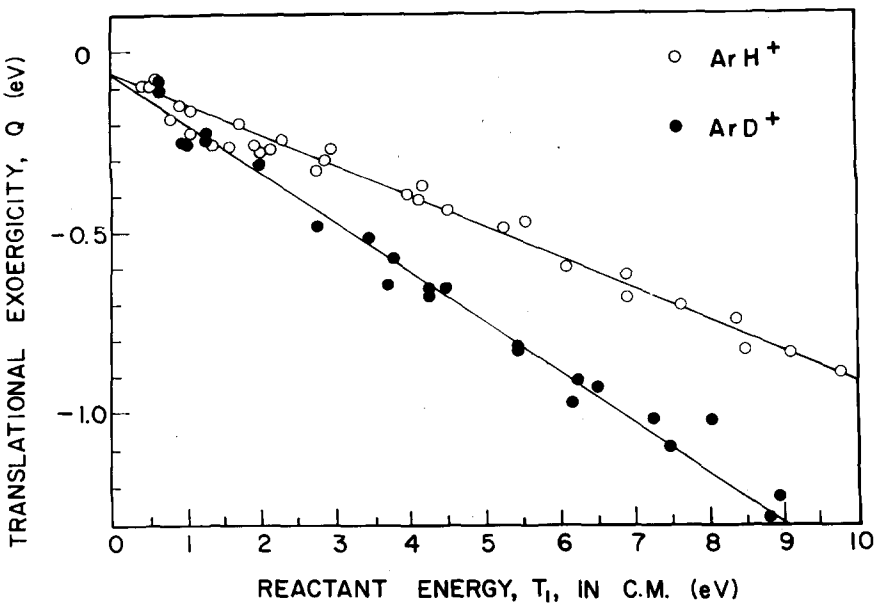

FIG. 10. Q vs T_1 for reaction of Ar^+ with CH_4 (○) and with CD_4 (●) over the energy range 0–10 eV c.m. The solid lines represent the best linear fit to the experimental data from a least squares analysis.

pected to apply. The straight lines represent a "best fit" to the experimental data, as obtained from a least squares analysis. Experimentally measured values for Q_0 and $(f-1)$ are listed in Table II, along with predictions of the spectator stripping model.

It is clear that the spectator stripping model, which predicts $Q_0 = 0$, consistently overestimates the translational energy of the reaction products by a nearly constant amount (~ 0.1 eV) although the predicted and observed slopes are in very good agreement.

The observation that $Q_0 < 0$ is unique, contrasting with the behavior of a number of hydrogenic transfer ion–molecule reactions studied by molecular beams[47] and high pressure mass spectrometric techniques.[48] In all reactions studied, there was a net increase in translational energy at the lowest collision energies ($Q_0 > 0$).

If product translation is presumed to arise from repulsive energy release as XY separates from Z,[46] the net decrease in translational energy observed for Reaction (2) suggests that the potential energy surface along the Y–Z coordinate has a positive slope resulting from XY–Z attraction. (That is, P' is negative.) This attraction produces a basin in the potential energy hypersurface from which the products can escape only with difficulty, particularly at the lowest collision energies. Direct reaction can occur only if the collision energy is high enough and the geometry of the collision such that the newly formed products retain sufficient momentum to escape from the potential basin and separate completely[34] [i.e., $f(P+T_1)$ must be greater in magnitude than P']. The existence of such a basin is consistent with Henglein's suggestions[17] and with the direct observation of $ArCH_4^+$ in high pressure mass spectrometric studies of $Ar-CH_4$ mixtures.[16]

The observed negative value for Q_0 implies that there is a critical value of the collision energy, $T_c = -Q_0/f$, below which the products are unable to separate because the final relative translational energy would be negative. With the values for Q_0 and f obtained from the least squares analysis of the data, this "stripping threshold" energy T_c equals 0.08 eV for Reaction (2a) and 0.07 eV for Reaction (2b). As reported previously, the excitation function for Reaction (2a) passes through a maximum at about 5 eV (c.m.) and decreases at lower collision energies, appearing to possess a threshold at ~ 0.1 eV.

The observed decrease in the reaction cross section at low collision energies and the failure to observe product distributions that are symmetric about the center of mass suggest that if an $ArCH_4^+$ intermediate complex is formed at low energies, the complex preferentially decomposes via reaction channels other than ArH^+ formation. Several oscillations of the complex may be required before ArH^+ can give the CH_3 a "clout" sufficient

TABLE II. Comparison of experiment with spectator stripping model.[a]

	$Ar^+ + CH_4$		$Ar^+ + CD_4$	
	Q_0	$(f-1)$	Q_0	$(f-1)$
1. Exptl. results	-0.075 ± 0.020	-0.081 ± 0.005	-0.060 ± 0.039	-0.142 ± 0.010
2. SS model	0	-0.085	0	-0.143

[a]See Eq. (17) of the text for the meaning of Q_0 and $(f-1)$. The experimental values reported were obtained from a least squares analysis of the data, and the uncertainties listed represent 95% confidence limits obtained from the least squares analysis.

This article is copyrighted as indicated in the article. Reuse of AIP content is subject to the terms at: http://scitation.aip.org/termsconditions. Downloaded to IP: 129.237.46.100 On: Thu, 11 Sep 2014 20:24:30

to effect complete separation. Competing with this energy transfer step are the dissociative charge transfer steps, Reactions (4) and (5). Our failure to detect ArH^+ at low energies, and the observation of CH_3^+ and CH_2^+ ions with velocity distributions peaked near the center of mass velocity[19] suggest that dissociative charge transfer is the preferred mode of decomposition of any collision complex that may be formed at low energies.

V. SUMMARY AND CONCLUSIONS

(1) Reaction (2) is dominated by a direct mechanism over the entire energy range studied, with no evidence for the production of ArH^+ via the decomposition of a long-lived collision complex. An important consequence to the finding that no strong coupling occurs is that statistical theory is inapplicable to this reaction.[49]

(2) The spectator stripping model, although providing a first approximation to the reaction dynamics, consistently overestimates the product translational energy (or, equivalently, underestimates product internal energy) by about 0.1 eV over the entire energy range 0–10 eV. This presumably stems from the model's failure to consider intermolecular forces. Circumstantial evidence is presented to support the hypothesis that little internal excitation of the methyl product occurs at collision energies less than 10 eV; at higher energies stabilization of the ionic product is assisted by the availability of energy sinks in the methyl product.

(3) The observation that product velocities are lower than expected (on the basis of the spectator stripping model) is consistent with the suggestion that the potential energy hypersurface contains a basin which hinders product separation. At very low collision energies (< 0.1 eV), this basin causes the reactants to undergo a lingering interaction and gives rise to a threshold for stripping. Decreased ArH^+ intensity in this energy region indicates that H atom abstraction is, at best, a minor channel for the decomposition of the $ArCH_4^+$ complex.

(4) The dynamics of the Ar^+–CH_4 reaction bear certain striking similarities to features observed for certain neutral–neutral reactions, principally those involving H atom abstraction from methane and other simple hydrocarbons by tritium or atomic flourine. These similarities suggest that certain general features may be common to a wide variety of simple transfer reactions.

ACKNOWLEDGMENTS

Acknowledgment is made to the donors of the Petroleum Research Fund, administered by the American Chemical Socity, for partial support of this research. Additional support was provided by the Research Corporation and by the University of Kansas General Research Fund. We would like to thank Professor Robert Sampson and the Kansas Geological Survey for providing the computer program used to construct the intensity contour diagrams.

*Present address: Naval Research Laboratory, Washington, D. C. 20375.

†Present address: Department of Chemistry, Emory University, Atlanta, GA.

‡Present address: Research Materials Laboratory, 2300 Van Buren Street, Topeka, KS.

[1] A. Henglein, K. Lacmann, and G. Jacobs, Ber. Bunsenges. Phys. Chem. 69, 279, 286, 292 (1965).

[2] R. L. Champion, L. D. Doverspike, and T. L. Bailey, J. Chem. Phys. 45, 4385 (1966).

[3] A. Ding, K. Lacmann, and A. Henglein, Ber. Bunsenges. Phys. Chem. 71, 596 (1967).

[4] R. D. Fink and J. S. King, J. Chem. Phys. 47, 1875 (1967).

[5] W. R. Gentry, E. A. Gislason, Y.-t. Lee, B. H. Mahan, and C.-w. Tsao, Discuss. Faraday Soc. 44, 137 (1967).

[6] W. R. Gentry, E. A. Gislason, B. H. Mahan, and C.-w. Tsao, J. Chem. Phys. 49, 3058 (1968).

[7] Z. Herman, J. Kerstetter, T. Rose, and R. Wolfgang, Discuss. Faraday Soc. 44, 123 (1967); J. Chem. Phys. 46, 2844 (1967).

[8] P. M. Hierl, Z. Herman, and R. Wolfgang, J. Chem. Phys. 53, 660 (1970).

[9] J. Kerstetter and R. Wolfgang, J. Chem. Phys. 53, 3765 (1970).

[10] R. E. Minturn, S. Datz, and R. L. Becker, J. Chem. Phys. 44, 1149 (1966).

[11] A. Henglein, K. Lacmann, and E. Knoll, J. Chem. Phys. 43, 1048 (1965).

[12] D. T. Chang and J. C. Light, J. Chem. Phys. 52, 5287 (1970).

[13] P. Hierl, Z. Herman, J. Kerstetter, and R. Wolfgang, J. Chem. Phys. 48, 4319 (1968).

[14] J. C. Light and S. Chan, J. Chem. Phys. 51, 1008 (1969).

[15] J. R. Wyatt, L. W. Strattan, S. C. Snyder, and P. M. Hierl, J. Chem. Phys. 60, 3702 (1974).

[16] F. H. Field, H. N. Head, and J. L. Franklin, J. Am. Chem. Soc. 84, 1118 (1962).

[17] (a) A. Ding, A. Henglein, D. Hyatt, and K. Lacmann, Z. Naturforsch. A 23, 2084 (1968); (b) A. Henglein, J. Chem. Phys. 53, 458 (1970).

[18] (a) E. Lindholm, Z. Naturforsch. A 9, 535 (1954); (b) C. E. Melton, J. Chem. Phys. 33, 647 (1960); (c) G. V. Karachevtsev, M. I. Markin, and V. L. Tal'roze, Kinet. Katal. 5, 377 (1964); (d) J. B. Homer, R. S. Lehrle, J. C. Robb, M. Takahasi, and D. W. Thomas, Advan. Mass Spectrom. 2, 503 (1963); (e) R. C. Bolden, R. S. Hemsworth, M. J. Shaw, and N. D. Twiddy, J. Phys. B 3, 45 (1970); (f) E. G. Jones and A. G. Harrison, Int. J. Mass Spectrom. Ion Phys. 6, 77 (1971); (g) M. T. Bowers and D. D. Elleman, Chem. Phys. Lett. 16, 486 (1972); (h) J. Gauglhofer and L. Kevan, Chem. Phys. Lett. 16, 492 (1972); (i) G. R. Hertel and W. R. Koski, J. Am. Chem. Soc. 87, 1696 (1965).

[19] A. J. Masson, K. Birkinshaw, and M. J. Henchman, J. Chem. Phys. 50, 4112 (1969).

[20] Z. Herman, J. D. Kerstetter, T. L. Rose, and R. Wolfgang, Rev. Sci. Instrum. 40, 538 (1969).

[21] C. F. Giese, Rev. Sci. Instrum. 30, 260 (1959).

[22] P. M. Hierl, L. W. Strattan, and J. R. Wyatt, Int. J. Mass Spectrom. Ion Phys. 10, 385 (1973).

[23] At higher electron energies, significant amounts of Ar^{++} are formed. These doubly charged ions, entering the collision chamber with twice the kinetic energy of the normal Ar^+ beam, undergo charge exchange with the target gas to form high energy Ar^+. Because of their excess kinetic energy, these charge exchange product ions form, on the high mass side of the $m/e = 40$ peak, a satellite peak which interferes with the ArH^+ mass peak.

[24] H. D. Hagstrum, Phys. Rev. 104, 309 (1956).

[25] (a) W. G. Rich, S. M. Bobbio, R. L. Champion, and L. D. Doverspike, Phys. Rev. A 4, 2253 (1971), (b) H. Mittman, H. P. Weise, A. Ding, and A. Henglein, Z. Naturforsch. A 26, 1112 (1971), (c) R. Klingbeil, J. Chem. Phys. 57, 1066

This article is copyrighted as indicated in the article. Reuse of AIP content is subject to the terms at: http://scitation.aip.org/termsconditions. Downloaded to IP: 129.237.46.100 On: Thu, 11 Sep 2014 20:24:30

(1972).
[26](a) A. C. Roach and P. J. Kuntz, Chem. Commun. 1970, 1336; (b) V. Sidis, J. Phys. B 5, 1517 (1972).
[27]K. Watanabe, J. Chem. 26, 542 (1957).
[28]These values are considerably more negative than the value of $\Delta H = -1.20$ eV reported (Ref. 7) for the thermo-equivalent reaction of Ar^+ with H_2. This discrepancy arises because the value $\Delta H = -1.20$ eV was based upon earlier and less accurate values of $D(Ar-H^+)$.
[29]R. Wolfgang and R. J. Cross, J. Phys. Chem. 73, 743 (1969).
[30]D. R. Herschbach, Discuss. Faraday Soc. 33, 149 (1962).
[31]Z. Herman, A. Lee, and R. Wolfgang, J. Chem. Phys. 51, 452 (1969).
[32]Such an explanation has been proposed to explain the back-scattered intensity found for the similar reaction of Ar^+ with H_2 and D_2 (Ref. 8).
[33](a) P. J. Kuntz, E. M. Nemeth, J. C. Polanyi, and W. H. Wong, J. Chem. Phys. 52, 4654 (1970); (b) D. L. Bunker and M. D. Pattengill, *ibid.* 53, 3041 (1970).
[34]J. C. Polanyi, Discuss. Faraday Soc. 44, 293 (1967).
[35]R. Wolfgang, Acc. Chem. Res. 3, 48 (1970).
[36]J. C. Tully, Z. Herman, and R. Wolfgang, J. Chem. Phys. 54, 1730 (1971).
[37]C. R. Iden, R. Liardon, and W. S. Koski, J. Chem. Phys. 56, 851 (1972).
[38]For example, the reaction $X + CH_4 \rightarrow HX + CH_3$ is nearly thermoneutral when X + Cl (Ref. 39), exothermic by 1.4 eV when $X \neq F$ (Ref. 40) and exothermic by 1.7 eV when $X = Ar^+$.
[39]H. O. Pritchard, J. B. Pyke, and A. F. Trotman-Dickenson, J. Am. Chem. Soc. 77, 2629 (1955).
[40]G. C. Fettis, J. H. Know, and A. F. Trotman-Dickenson, J. Chem. Soc. 1960, 1064.
[41](a) K. L. Kompa and G. C. Pimentel, J. Chem. Phys. 47, 857 (1967), (b) K. L. Kompa, J. H. Parker, and G. C. Pimentel, *ibid.* 49, 4257 (1968), (c) J. H. Parker and G. C. Pimentel, *ibid.* 48, 5273 (1968), (d) J. H. Parker and G. C. Pimentel, *ibid.* 51, 91 (1969), (e) O. D. Krogh and G. C. Pimentel, *ibid.* 56, 969 (1972).
[42](a) T. P. Schafer, P. E. Siska, J. M. Parson, F. R. Tully, Y. C. Wong, and Y. T. Lee, J. Chem. Phys. 53, 3385 (1970), (b) J. M. Parson and Y. T. Lee, *ibid.* 56, 4658 (1972).
[43]E. A. Gislason, B. H. Mahan, C. W. Tsao, and A. S. Werner, J. Chem. Phys. 50, 142 (1969).
[44]F. T. Smith, J. Chem. Phys. 31, 1352 (1959).
[45]D. L. Bunker, Nature 194, 1277 (1962).
[46]See, for example, J. C. Polanyi, Acc. Chem. Res. 5, 161 (1972).
[47]See, for example, C. M. Connally and E. A. Gislason, Chem. Phys. Lett. 14, 103 (1972), and references cited therein.
[48]J. L. Franklin and M. A. Haney, J. Phys. Chem. 73, 2857 (1969).
[49](a) V. L. Tal'roze and G. V. Karachevtsev, Adv. Mass Spectrom. 3, 211 (1966); (b) J. C. Light Discuss. Faraday Soc. 44, 80 (1967).

This article is copyrighted as indicated in the article. Reuse of AIP content is subject to the terms at: http://scitation.aip.org/termsconditions. Downloaded to IP: 129.237.46.100 On: Thu, 11 Sep 2014 20:24:30